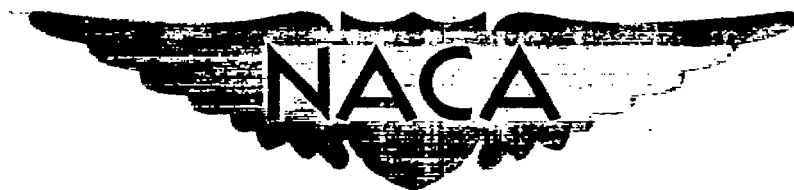


UNCLASSIFIED



# RESEARCH MEMORANDUM

INVESTIGATION OF THE I-40 JET-PROPULSION ENGINE IN THE  
CLEVELAND ALTITUDE WIND TUNNEL

III - ANALYSIS OF TURBINE PERFORMANCE AND EFFECT  
OF TAIL-PIPE DESIGN ON ENGINE PERFORMANCE

By Richard P. Krebs and Frederick C. Foshag

Flight Propulsion Research Laboratory  
Cleveland, Ohio

CLASSIFICATION CANCELLED

Authority J. W. Crawley Date 12/14/53

By DH-1-19-54 See NACA DOCUMENT  
RF 1949

This document contains classified information affecting the National Defense of the United States within the meaning of the Espionage Act, USC 50:81 and 82. Its transmission or the revelation of its contents in any manner to an unauthorized person is prohibited by law. Information so classified may be imparted only to persons in the military and naval services of the United States, appropriate civilian officers and employees of the Federal Government who have a legitimate interest therein, and to United States citizens of known loyalty and discretion who of necessity must be informed thereof.



NATIONAL ADVISORY COMMITTEE  
FOR AERONAUTICS

WASHINGTON  
August 26, 1948

NACA LIBRARY  
AERONAUTICAL LABORATORY  
1200 Field Bldg.

UNCLASSIFIED

NATIONAL ADVISORY COMMITTEE FOR AERONAUTICS

RESEARCH MEMORANDUMINVESTIGATION OF THE I-# JET-PROPULSION ENGINE IN THE  
CLEVELAND ALTITUDE WIND TUNNELIII - ANALYSIS OF TURBINE PERFORMANCE AND EFFECT  
OF TAIL-PIPE DESIGN ON ENGINE PERFORMANCE

By Richard P. Krebs and Frederick C. Foshag

## SUMMARY

Turbine-performance characteristics of an I-40 jet-propulsion engine installed in an airplane fuselage were determined. A comparison of engine performance with three different tail pipes is also presented. The investigation was conducted in the Cleveland altitude wind tunnel over a range of simulated altitudes from 10,000 to 40,000 feet and a range of ram pressure ratios from 0.98 to 1.76.

Turbine characteristics are presented as functions of turbine pressure ratio, corrected gas flow, and corrected turbine speed. Changes in corrected net thrust, corrected net thrust horsepower, and specific fuel consumption based on net thrust horsepower with three different tail pipes are discussed.

A maximum turbine efficiency of approximately 0.835 was obtained. This efficiency is somewhat lower than the true turbine efficiency, inasmuch as the bearing friction, accessories drive, and tail-pipe losses have been charged against the turbine. Turbine efficiency was unaffected by changes in altitude or the tail-pipe designs but varied with changes in ram pressure ratio.

The most satisfactory engine performance was obtained with a constant-diameter tail pipe having a short nozzle at the outlet.

## INTRODUCTION

An investigation has been conducted on an I-40 jet-propulsion engine in the Cleveland altitude wind tunnel. Reference 1 contains a description of the engine and its installation in the tunnel and

UNCLASSIFIED

a summary of the engine performance characteristics. The compressor performance is analyzed in reference 2.

The investigation was conducted over a range of simulated altitudes from 10,000 to 40,000 feet and a range of ram pressure ratios from 0.98 to 1.76. These ram pressure ratios correspond to true airspeeds from 0 to approximately 650 miles per hour.

Changes in turbine operation brought about by changes in altitude, ram pressure ratio, and tail-pipe configuration are analyzed. Performance curves for the turbine, which cover only the range of conditions encountered by the turbine operating in the jet-propulsion engine, are presented. A comparison of engine performance with three different tail pipes at two ram pressure ratios is made.

#### DESCRIPTION OF TURBINE AND TAIL PIPES

The I-40-3 jet-propulsion engine is equipped with a single-stage impulse turbine (fig. 1). The turbine drives the compressor at a maximum speed of 11,500 rpm.

The turbine rotor has an outside diameter of 25.95 inches. It is overhung at the rear of the shaft, which is supported by a roller bearing about 4 inches ahead of the center plane of the rotor and a ball thrust bearing at the front. Both bearings are lubricated by jets of oil pumped from the accessory section. The rotor-disk diameter is 17.835 inches. The disk thickness decreases from 4.25 inches at the shaft to approximately 2.29 inches at the periphery. Fifty-four solid square-ended blades  $4\frac{1}{16}$  inches long are dovetailed to the disk. The radial tip clearance for the wheel is about 0.06 inch and the axial clearance between the leading edge of the rotor blades and the trailing edge of the nozzle blades varies from 0.80 inch at the root to 0.88 inch at the tip.

A cooling fan on the forward face of the turbine rotor is supplied with air from the rear compressor inlet. (See fig. 2.) The air passes rearward over the outside of the turbine support casing and the rear bearing then radially outward through the fan and the diffuser. After cooling the rotor, the air turns and passes forward beneath the combustion chambers and outward between them. The discharged air does not enter the tail-pipe gas flow. The cooling air constitutes about 2 percent of the air flow through the engine at maximum speed.

641 r

In the airplane fuselage used the tail pipe extends from the exhaust cone to the rear extremity of the fuselage. For this investigation an instrumented ring was connected to the exit of the exhaust cone. The tail-pipe was connected to the instrumented ring by a detachable clamp ring end was supported in the fuselage rear section on rollers that rode on tracks located on both sides of the fuselage. Tail pipes could be easily changed after the fuselage rear section had been removed.

**Engine-performance** runs were made with three tailpipes of similar construction but slightly different dimensions. The tail-pipe stock was **0.03-inch** stainless steel. The tail-pipe insulation consisted of 0.01-inch **14-mesh** stainless-steel screen longitudinally corrugated and two layers of **0.004-inch** aluminum foil pressed **into the corrugations**. The screen and foil were held in place by **1/8-inch** asbestos-covered wire **spirally** wrapped around the tail pipe with a pitch of 1 inch.

The three tail pipes, designated 1, 2, and 3, had the following physical characteristics (fig. 3):

1. Tailpipe **1** conformed to the standard production tail pipe except that it was 4 inches shorter to **accommodate** the instrumented ring. It was 93.31 inches long and had a constant taper from a diameter of approximately 21 inches at the entrance end to 19 inches at the outlet end.
2. Tail pipe 2 was similar to 1 except for a 2-inch extension **on** the outlet end, which reduced the exit diameter to 18.8 inches.
3. Tailpipe 3 was an **experimental** model. It had the **same** outlet area as tail pipe 1, but consisted of a **21-inch-diameter** section 86.12 inches long followed by a nozzle 7.19 inches long, which reduced the diameter to 19 inches at the outlet.

#### INSTRUMENTATION

The instrumentation used to obtain the data presented was installed at the stations shown **in** figure 2. All of the measurements were made by unshielded **instruments** except where noted. Details **of the instrumentation** at these stations were as follows:

Total pressure at station 2 was measured by 14 shielded **total-pressure** tubes at the front compressor inlet and 28 shielded tubes at the rear **compressor inlet**. Temperature was measured by 7 **thermo-**

at the rear compressor inlet. **Temperature** was measured by 7 thermocouples at **the** front compressor inlet and 14 thermocouples at the rear **compressor** inlet. Compressor-inlet instrumentation was located on **an** imaginary cylindrical surface, which was 6 inches greater in diameter than the inlet screen (fig. 2), and as near as possible to the axial center of the inlet.

At station 5 the **turbine-inlet** total pressure was measured by total-pressure tubes located in three of **the** burners. The tubes were located approximately midway between the center line and the outside surface of the burner and about 2.5 inches from the forward edge of the nozzle diaphragm. Thermocouples were inserted in each burner to determine which burners were lighted.

Data from instrumentation at station 6 have not been used herein because they were apparently in error. The **error** was caused by excessive swirl and by radiation from the hot turbine gases.

The diffuser vanes in the exhaust cone removed most of the swirl at the tail-pipe-nozzle outlet and the thermocouples in the tail-pipe-nozzle **outlet were** sufficiently remote to be unaffected by radiation from the hot gases. The instrumentation at station 8 consisted of 18 total-pressure tubes, 3 static-pressure tubes, 4 static wall orifices, and 10 thermocouples. Tail pipe 1 was also instrumented with 4 additional static wall orifices. All of the instrumentation with the exception of the wall orifices was carried on a single vertical rake fastened to the end of the tail pipe. The plane of the instrumentation was 1 inch inside tail pipes 1 and 2 and **3/8** inch inside tail pipe 3.

#### RANGE OF INVESTIGATIONS

Engine-performance runs with tail pipe 1 were conducted over a range of simulated altitudes from 10,000 to 40,000 feet and over a range of ram pressure ratios from 0.98 to 1.76. Comparative runs with tail pipes 2 and 3 were conducted at a simulated altitude of **20,000** feet at ram pressure ratios of 1.03 and 1.27. **Ram** pressure ratio is defined as the ratio of the average total pressure at the front and the rear compressor inlets to the free-stream static pressure in the tunnel. In these runs the temperature of the inlet air could not be maintained to simulate precisely altitude conditions.

**SYMBOLS**

The following symbols' are used in the **calculations:**

<b>A</b>	cross-sectional area, square feet
<b>F<sub>j</sub></b>	jet thrust, pounds
<b>F<sub>n</sub></b>	net thrust, pounds
<b>g</b>	ratio of absolute to gravitational units, (32.17)
<b>K<sub>g</sub></b>	gas-flow calibration factor for tail-pipe-nozzle outlet rake, (0.964)
<b>M<sub>a</sub></b>	mass air flow, slugs per second
<b>N</b>	engine speed, rpm
<b>P</b>	total pressure, pounds per <b>square</b> foot
<b>p</b>	static pressure, pounds per square foot
<b>R</b>	gas constant (at elevated temperatures), foot-pounds per pound <b>°R</b> (53.86)
<b>T</b>	total temperature, <b>°R</b>
<b>T<sub>i</sub></b>	indicated temperature, <b>°R</b>
<b>t</b>	static temperature, <b>°R</b>
<b>thp</b>	net thrust horsepower
<b>u</b>	turbine-rotor tip speed, feet per second
<b>V<sub>0</sub></b>	effective airspeed, feet per second
<b>v</b>	turbine-nozzle jet speed, feet per second
<b>W<sub>f</sub></b>	fuel flow, pounds per hour
<b>W<sub>g</sub></b>	gas flow, pounds per second
<b>a</b>	thermocouple <b>impact-recovery</b> factor, (0.86)
<b>γ</b>	ratio of specific heats

- $\delta$  pressure correction factor,  $P/2116$ , local **total** pressure divided by **NACA** standard atmospheric pressure at sea level
- $\eta_t$  turbine efficiency
- $\theta$  temperature correction factor,  $\gamma T/1.4 \times 519$ , product of local temperature and  $\gamma$  divided by the product of temperature and  $\gamma$  for air at **NACA** standard atmospheric conditions **at sea level**

Subscripts:

- 0 free stream
- 2 compressor inlet (average of measurements at front and rear)
- 5 turbine inlet
- 8 tail-pipe-nozzle outlet
- t turbine
- x annular increment of **area** in tail-pipe-nozzle outlet

#### METHODS OF CALCULATION

Efficiency. - Turbine efficiency was calculated by the following equation:

$$\eta_t = \frac{1 - \frac{T_8}{T_5}}{1 - \left(\frac{P_8}{P_5}\right)^{\frac{\gamma-1}{\gamma}}}$$

This efficiency is based on the total-pressure drop **across** the turbine. Pressure losses in the tail pipe **are** charged to the turbine because tail-pipe-nozzle outlet measurements **were** used instead of corresponding turbine-outlet measurements.

Because the thermocouples at station 5 were subjected to the radiation from the hot burner gases, they were not satisfactory for the computation of  $T_5$ . An indirect method of determining  $T_5$  was

therefore **used**. The enthalpy drop across the turbine was assumed equal to the enthalpy rise across the compressor. The **value** of  $T_5$  was computed from  $T_3$  and the turbine enthalpy drop by means of the charts in reference 3. The fuel (kerosene) had a hydrogen-carbon ratio of 0.175 and a lower heating value of 18,600 Btu per pound.

The **value** of  $\gamma$  was determined from a curve relating  $\gamma$  and **temperature** at a constant fuel-air ratio of 0.02 and a burner efficiency of 70 percent. The temperature used was the average of  $T_5$  and  $T_3$ . The error in turbine efficiency introduced by considering fuel-air ratio and burner efficiency constant in computing  $\gamma$  was less than 1/2 percent.

The work output of the turbine should include the work put into the compressor, the compressor thermal-radiation losses, and the work required to overcome bearing friction and to drive the accessories. In the computation of the work output of the turbine, however, only the work put into the compressor was considered. Although the resultant efficiency value is lower than the actual adiabatic efficiency of the turbine, it is considered sufficiently accurate to justify comparisons among the efficiencies for **changes** in altitude, **ram pressure** ratio, and tail pipe.

Gas flow. - Gas **flow was determined from measurements** taken at the tail-pipe-nozzle outlet, station 8. Inasmuch as the total and static pressures and indicated **temperatures** varied across the tail pipe, the area at the plane of survey was divided into a series of **annuli** and the gas flow through each **annulus** was calculated. A summation of the **incremental** values determined the **total** gas flow through the engine. The following equation was used:

$$W_g = \left[ K_g P_8 \sqrt{\frac{2\gamma g}{(\gamma-1)R}} \sum A_x \sqrt{\frac{\left(\frac{P_x}{P_x}\right)^{\frac{\gamma-1}{\gamma}} - 1}{T_{1,x}} + \alpha \left[\left(\frac{P_x}{P_x}\right)^{\frac{\gamma-1}{\gamma}} - 1\right]^2} \right] C$$

where C is an area-correction factor dependent on temperature. This gas-flow equation is derived in reference 1.

Temperatures. - Tail-pipe-nozzle outlet static temperature was calculated from indicated temperature by the use of the equation

$$t_8 = \frac{T_{1,8}}{1 + \alpha \left[ \left( \frac{P_8}{P_8} \right)^{\frac{\gamma-1}{\gamma}} - 1 \right]}$$

Tail-pipe-nozzle outlet total temperature was computed by

$$T_8 = t_8 \left( \frac{P_8}{P_8} \right)^{\frac{\gamma-1}{\gamma}}$$

Effective airspeed. - The calculation for effective airspeed was based on the assumption of **100-percent ram** efficiency in the inlet duct. The effective airspeed in terms of compressor-inlet values is

$$V_0 = \sqrt{\frac{2\gamma gR}{\gamma-1} t_0 \left[ \left( \frac{P_2}{P_0} \right)^{\frac{\gamma-1}{\gamma}} - 1 \right]}$$

Net thrust. - Net thrust was determined by subtracting the initial free-stream momentum of the air from the jet thrust.

$$F_n = F_j - M_a V_0$$

Net thrust horsepower. - Net thrust horsepower was calculated from the net thrust and effective airspeed by the following relation:

$$\text{thp} = \frac{F_n V_0}{550}$$

## RESULTS AND DISCUSSION

### Method of Presentation

The data are presented with the aid of corrected coordinates. The use of corrected coordinates in jet-propulsion-engine analysis is discussed in references 4 and 5. Two of **these** coordinates,

corrected turbine speed  $N/\sqrt{\theta_5}$  and corrected gas flow  $\frac{W_g \sqrt{\theta_5}}{\delta_5 \gamma_5 / 1.4}$ ,

as well as turbine pressure ratio  $P_5/P_8$ , are used in **describing** the turbine performance. Corrected net thrust  $F_n/\delta_2$  and corrected net thrust horsepower  $thp/\delta_2 \sqrt{\theta_2}$  are used in the tail-pipe comparison.

The coordinate  $u/v$  usually used in the **presentation** of turbine data is not used because the **range** of  $u/v$  for all engine operating conditions was only between 0.45 and 0.51. The turbine operating line used is defined as the plot of turbine total-pressure ratio against corrected gas flow. A jet-propulsion **engine** has a single turbine operating line if secondary effects such as **changes** in specific heat and Reynolds number are neglected.

### Turbine Performance

Turbine pressure ratio is plotted against corrected gas flow **and** corrected turbine speed for several altitudes and **ram** pressure ratios with tail pipe 1 in figures 4 and 5, respectively. Although these data show that altitude and ram pressure ratio have no appreciable effect on the two plots, a more complete **analysis** of 'additional data taken with tail pipe 1 showed **an** altitude effect on the operating line. From the derivation of corrected gas flow given in reference 5, the assumption was made that the gas flow corrected to turbine-inlet conditions would be constant for **turbine** pressure ratios exceeding 1.8. Accordingly, **all** corrected gas flows corresponding to turbine pressure ratios above the critical turbine pressure ratio for several ram pressure ratios for each altitude were averaged together. This procedure was based on the assumption that changes in **ram** pressure ratio had no effect on the turbine **operating** line. The results of this averaging process are presented in the following table:

Altitude (ft)	-Average corrected gas flow (lb/sec)
10,000	42.04
20,000	41.89
30,000	41.59
40,000	41.37

This table definitely indicates that the turbine operating line shifts toward lower corrected gas flows as the altitude increases

Turbine efficiency for several altitudes is plotted in figure 6 as a function of turbine pressure ratio at a ram pressure ratio of 0.98. This figure shows that the turbine efficiency is independent of altitude.

Turbine efficiency for various ram pressure ratios is plotted against turbine pressure ratio and corrected turbine speed in figure 7. Data points have been omitted in order not to obscure the curves.

A maximum turbine efficiency of about 0.835 was obtained at a ram pressure ratio between 1.1 and 1.2 with a turbine pressure ratio between 1.6 and 2.0, corresponding to a range of corrected turbine speeds from 4400 to 5400 rpm. This efficiency is somewhat lower than the true turbine efficiency, inasmuch as the bearing friction, accessories drive, and tail-pipe losses have been charged against the turbine. The engine speed in this region of maximum turbine efficiency is between 6600 and 8700 rpm. In this range of turbine operation the curves are fairly flat for ram pressure ratios of 1.09 and 1.21. The curves for ram pressure ratios of 0.98, 1.03, and 1.76 are steeper than the curves for 1.09 and 1.21 ram pressure ratios and peak at a turbine pressure ratio of about 2.25.

The values of peak turbine efficiency and turbine efficiency at maximum engine speed for six different ram pressure ratios are tabulated as follows:

Ram pressure ratio	Peak turbine efficiency	Turbine efficiency at maximum engine speed
0.98	0.82	0.805
1.03	.82	.81
1.09	.835	.82
1.21	.835	.805
1.38	.83	.805
1.76	.81	.80

Cross plots taken from figure 7 of turbine efficiency as a function of ram pressure ratio for three turbine pressure ratios that would prevail during flight operation are shown in figure 8. The variation of turbine efficiency with ram pressure ratio is assumed to be the result of changes in compressor performance. The compressor efficiency is greatly affected by changes in ram pressure ratio, especially at low engine speeds. (See reference 2.) The change in compressor efficiency alters the flow pattern of the

compressor-discharge air. These flow modifications may persist through the combustion **chambers and** influence the turbine efficiency.

#### Effect of Tail-Pipe Design on Engine Performance

The turbine operating line and a plot of turbine pressure ratio against corrected turbine speed for the three tail pipes are shown in figure 9. The data were taken at **an** altitude of **20,000** feet and a ram pressure ratio of 1.03. The turbine operating line is altered by a **change** in tailpipe. The data indicate that corrected gas flows are higher with tail pipes **2 and** 3 than with tail pipe 1. The turbine pressure ratio plotted against corrected turbine speed is the **same** for the three tailpipes.

**Turbine** efficiency is plotted against turbine pressure ratio at several **altitudes and** a ram pressure ratio of 1.03 for tail pipes 2 and 3 in figure 10. These curves match the efficiency curve at a **ram** pressure ratio of 1.03 for tail pipe 1 shown **in** figure 7 except for a slight decrease in **turbine** efficiency with tail pipe 2 at low turbine pressure ratios.

An over-all engine-performance **comparison** with the three tail pipes was made at **ram** pressure ratios of 1.03 and 1.27. Corrected net thrust is plotted against corrected engine speed for the three tailpipes at a **simulated altitude** of 20,000 feet in figure 11. Because no data were available for tail pipe 1 at a ram pressure ratio of 1.27, the curve shown in figure 11 for this tailpipe was obtained by cross-plotting and interpolating data from other ram pressure ratios. The engine operating at **maximum** engine speed (**11,500 rpm**) corresponding to a corrected turbine speed of about **12,000 rpm** produces **5 $\frac{1}{2}$**  percent more corrected net thrust with tail pipe 3 than with tail pipe 1.

In figure 12 corrected net thrust horsepower is plotted against specific fuel consumption based on net thrust horsepower. Over the entire operating **range** for a **ram** pressure ratio of 1.03 tail pipe 3 gives the **most** economical fuel consumption. At a ram pressure ratio of 1.27 and a corrected net thrust horsepower above 2500, tail pipe 3 maintains a similar advantage over the two other tail pipes. Tail pipe 2 gives **an engine performance** generally intermediate to those obtained **with** tail pipes 1 and 3.

## SUMMARY OF RESULTS

From an investigation of the I-40 jet-propulsion engine, the following results were obtained on the turbine performance and the effect on engine performance of three different tail pipes:

1. A maximum turbine efficiency of about 0.835 was obtained at a ram pressure ratio between 1.1 and 1.2 with a turbine pressure ratio between 1.6 and 2.0. This efficiency is somewhat lower than the true turbine efficiency, inasmuch as the bearing friction, accessories drive, and tail-pipe losses have **been** charged against the turbine. The maximum turbine efficiency obtained at maximum engine speed was 0.82 at a ram pressure ratio of 1.1.

2. Turbine efficiency was independent of changes in altitude and was inappreciably affected by **changesintail-pipedesign** but varied with changes in ram pressure ratio.

3. A constant-diameter tail pipe, having a short nozzle at the outlet, gave the generally most satisfactory corrected net thrust and fuel **economy**.

Flight Propulsion Research Laboratory,  
National Advisory Committee for **Aeronautics**,  
Cleveland, Ohio.

**REFERENCES**

1. **Gendler, Stanley L., and Koffel, William K.**: Investigation of the I-40 Jet-Propulsion Engine in the Cleveland Altitude Wind Tunnel. I - Performance and Windmilling Drag Characteristics. NACA RM No. **ESG02**, 1948.
2. Dietz, Robert O., Jr., and **Geisenkeyner, Robert M.**: Investigation of the I-40 Jet Propulsion Engine in the Cleveland Altitude Wind Tunnel. II - Analysis of Compressor Performance Characteristics. NACA RM No. **ESG02a**, 1948.
3. Turner, L. Richard, and Lord, Albert M.: Thermodynamic Charts for the Computation of Combustion and Mixture Temperatures at Constant Pressure. NACA TN No. **1086**, 1946.
4. Sanders, Newell D.: Performance Parameters for Jet-Propulsion Engines. NACA TN No. **1106**, 1946.

5. **Krebs, Richard P., and Hensley, Reece V.:** Altitude-Wind-Tunnel Investigation of a **4000-Pound-Thrust** Axial-Flow Turbojet Engine. **V** - Analysis of Turbine Performance. NACA RM No. **ESF09d**, 1948.

•

•

•

•

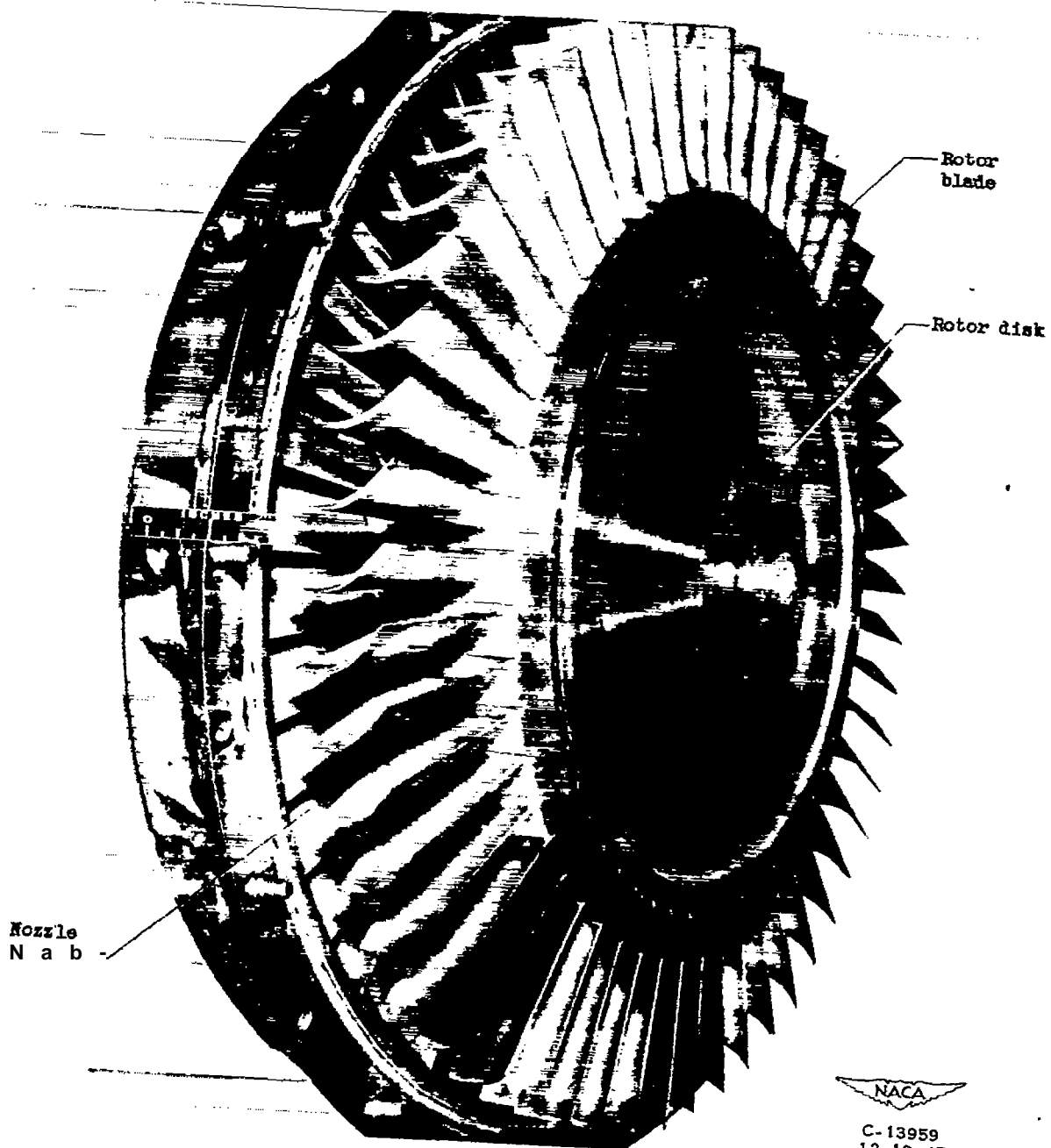


Figure 1. - Single-stage impulse turbine of I-40 jet-propulsion engine.

•

•

•

•

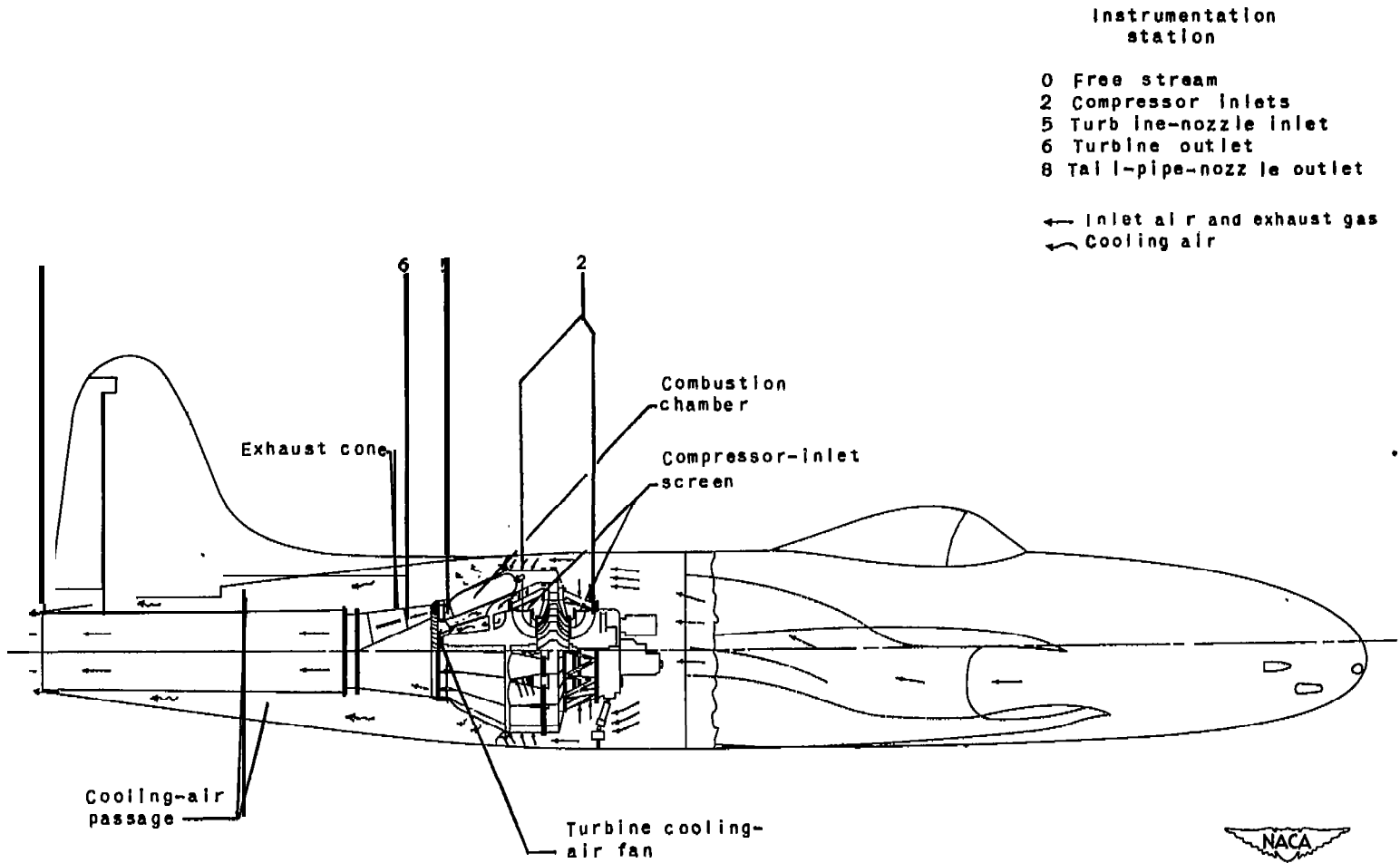
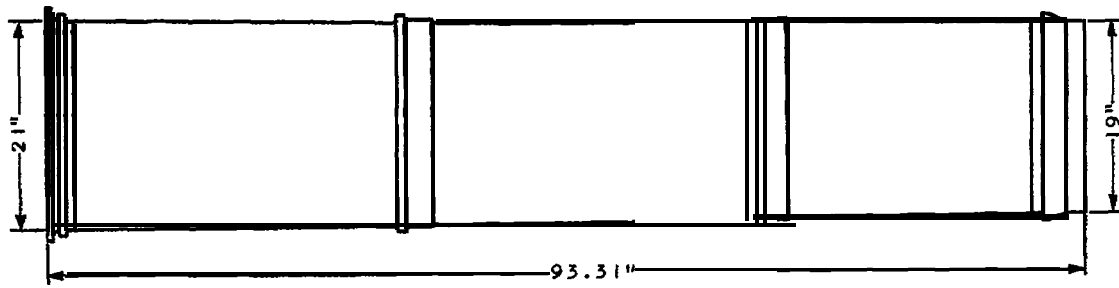
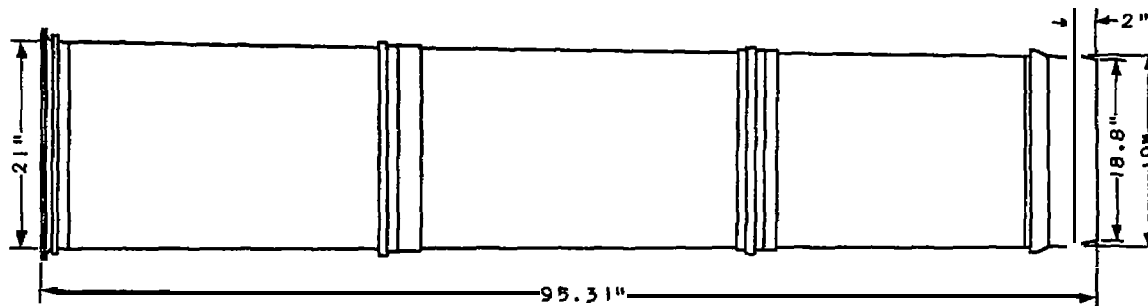


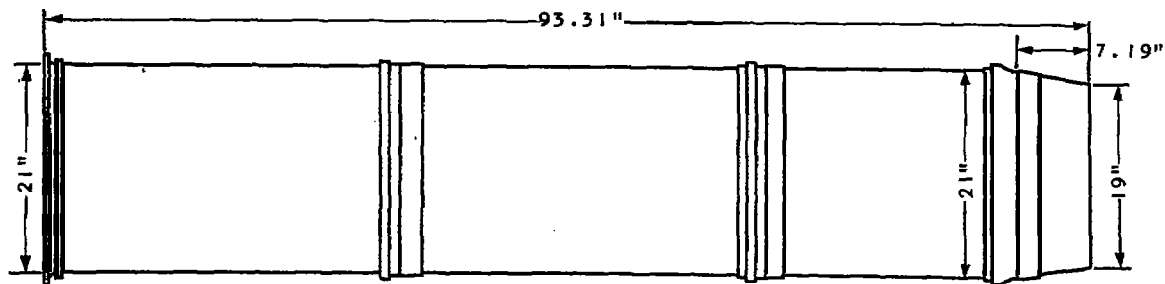
Figure 2. - The I-40 jet-propulsion engine installed in airplane fuselage.



Tail pipe 1



Tail pipe 2



Tail pipe 3

Figure 3. - Elevation of three tail pipes used in investigations of I-40 jet-propulsion engine.

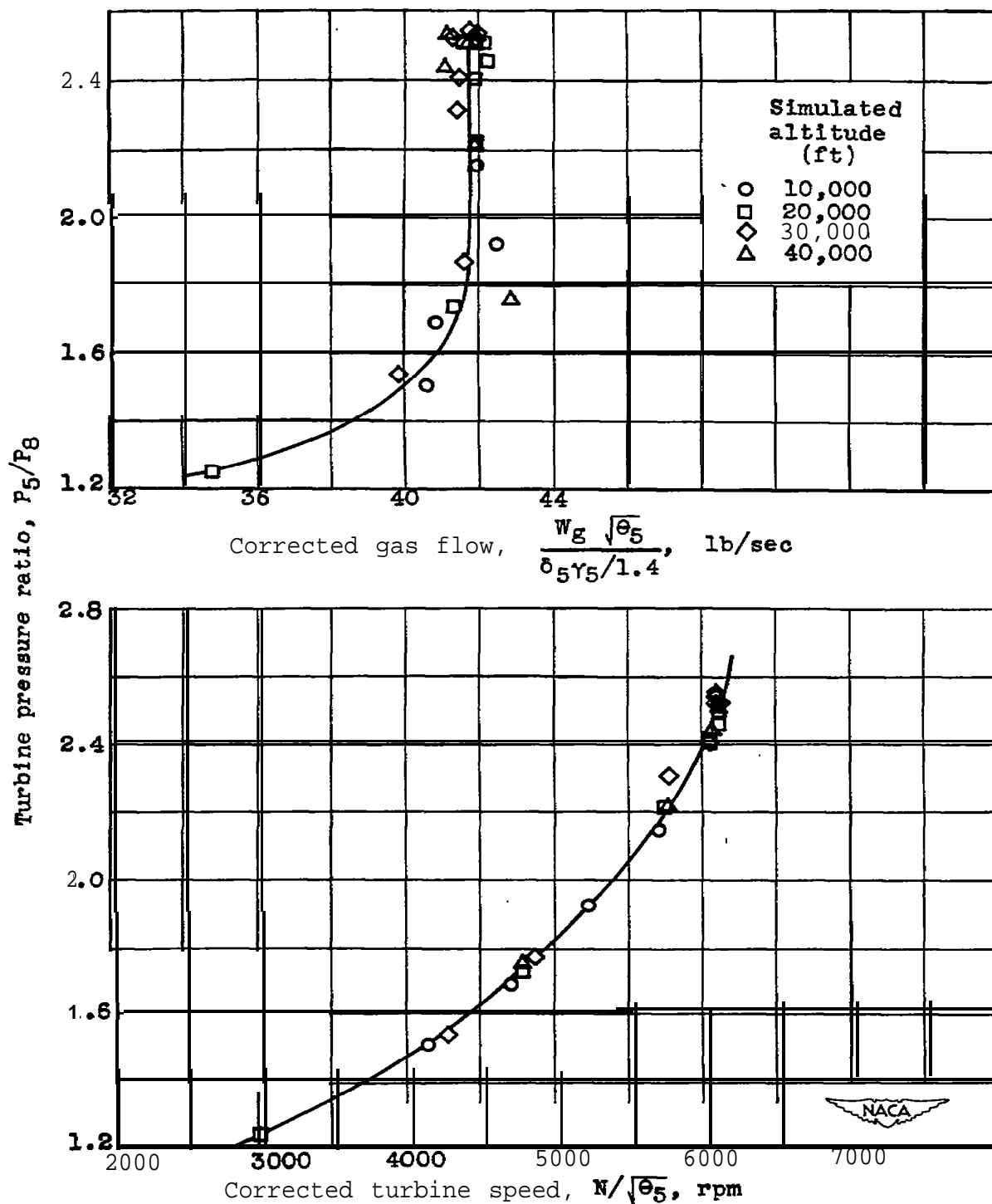


Figure 4.- Turbine operating line and plot of turbine pressure ratio against corrected turbine speed for several altitudes at ramp pressure ratio of 2.01 with tail pipe 1. Gas flow and turbine speed corrected to NACA standard atmospheric conditions at sea level.

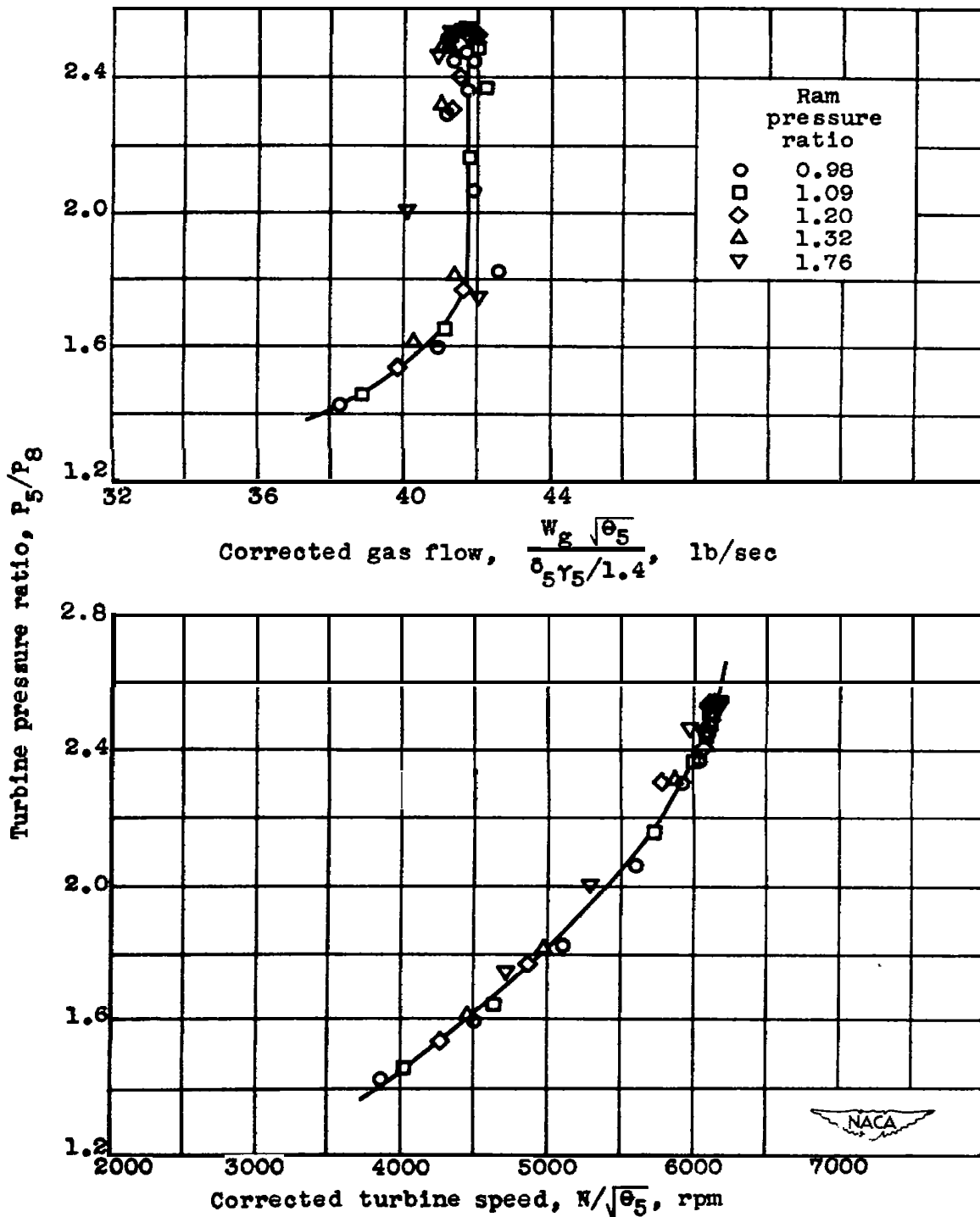


Figure 5.- Turbine operating line and plot of turbine pressure ratio against corrected turbine speed for several ram pressure ratios at simulated altitude of 30,000 feet with tail pipe 1. Gas flow and turbine speed *corrected* to NACA standard atmospheric conditions at sea level.

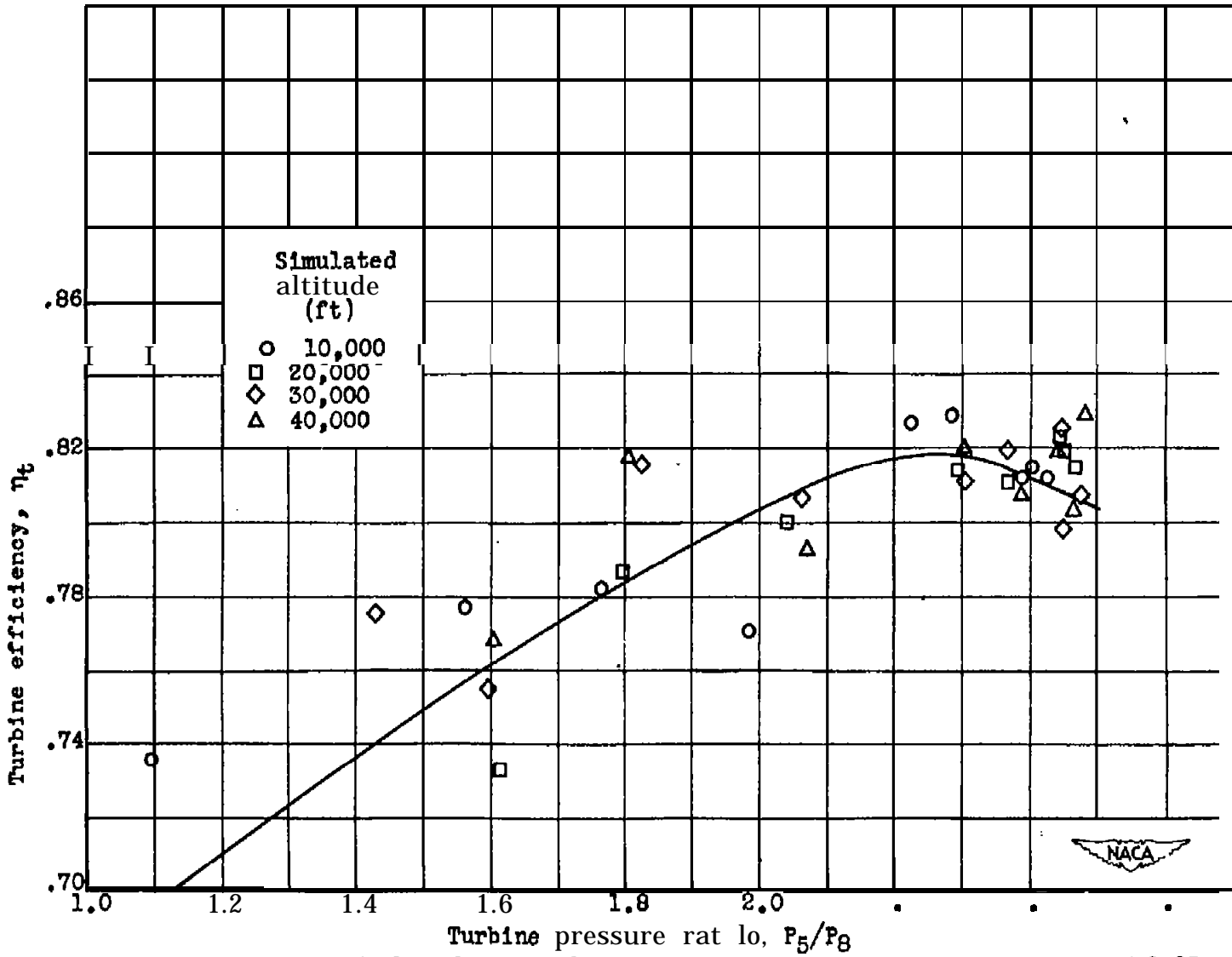


Figure 6.- Effect of altitude on turbine efficiency at a ram pressure ratio of 0.98 with tell pipe 1.

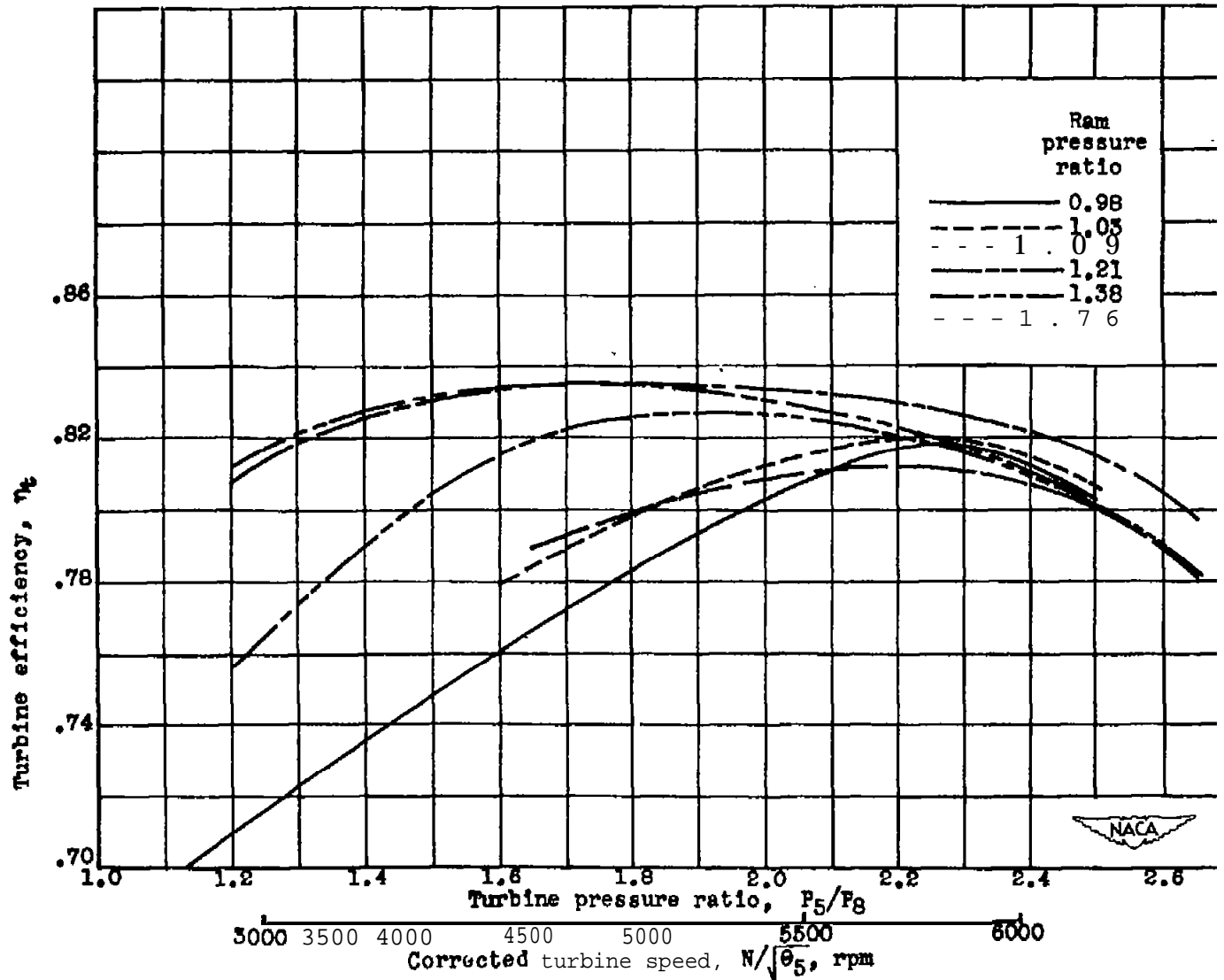


Figure 7.- Effect of ram pressure ratio on turbine efficiency with tail pipe 1. Turbine speed corrected to NACA standard atmospheric conditions at sea level.

641

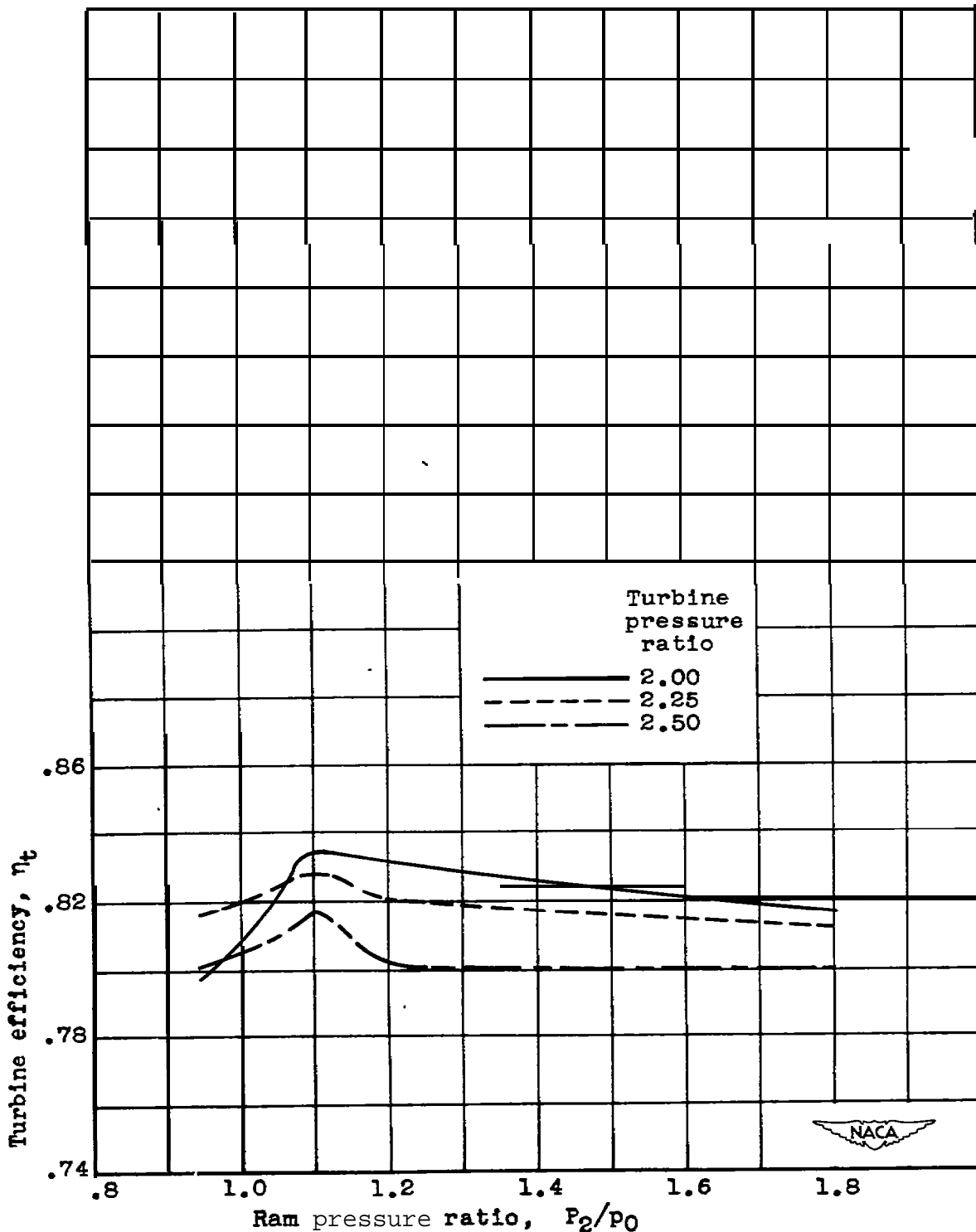


Figure 8.- Turbine efficiency as function of ram pressure ratio for three values of turbine pressure ratio with tail pipe 1,

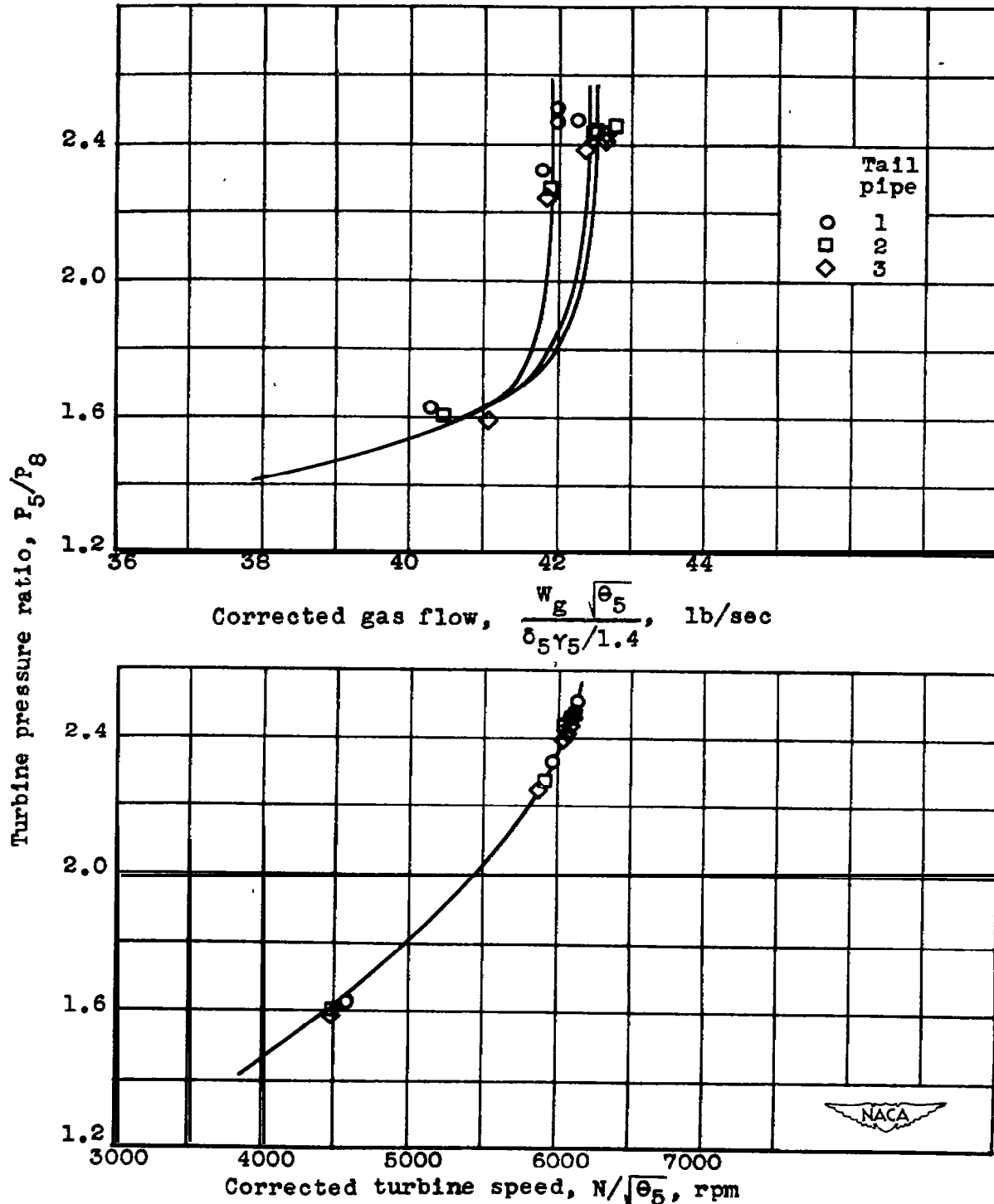
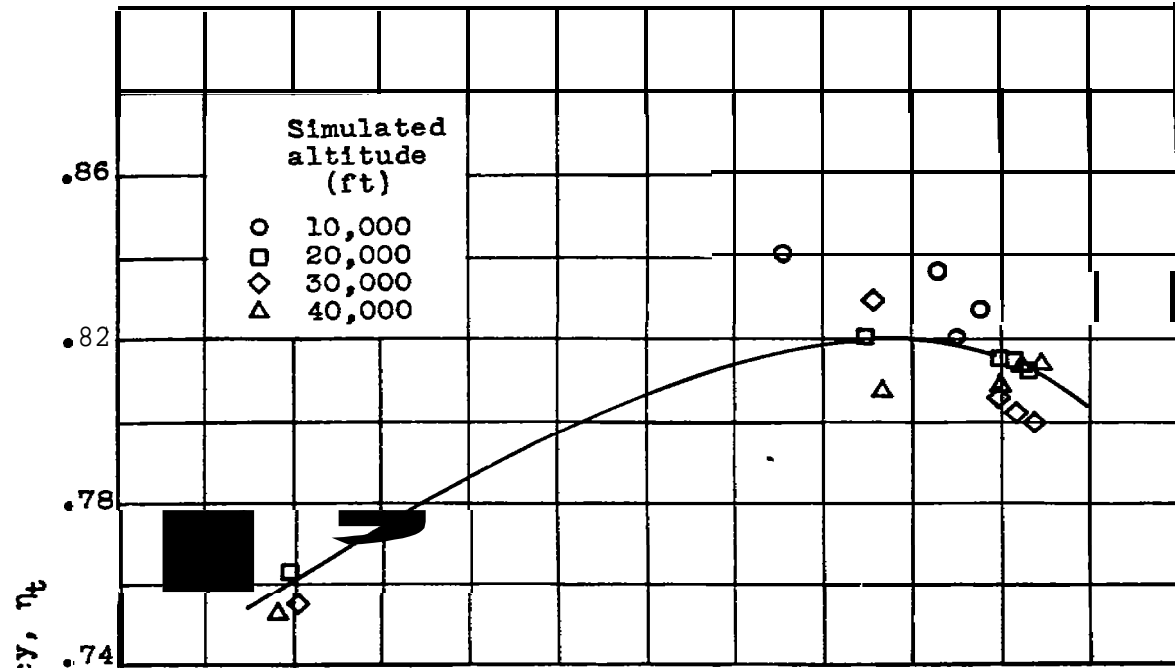
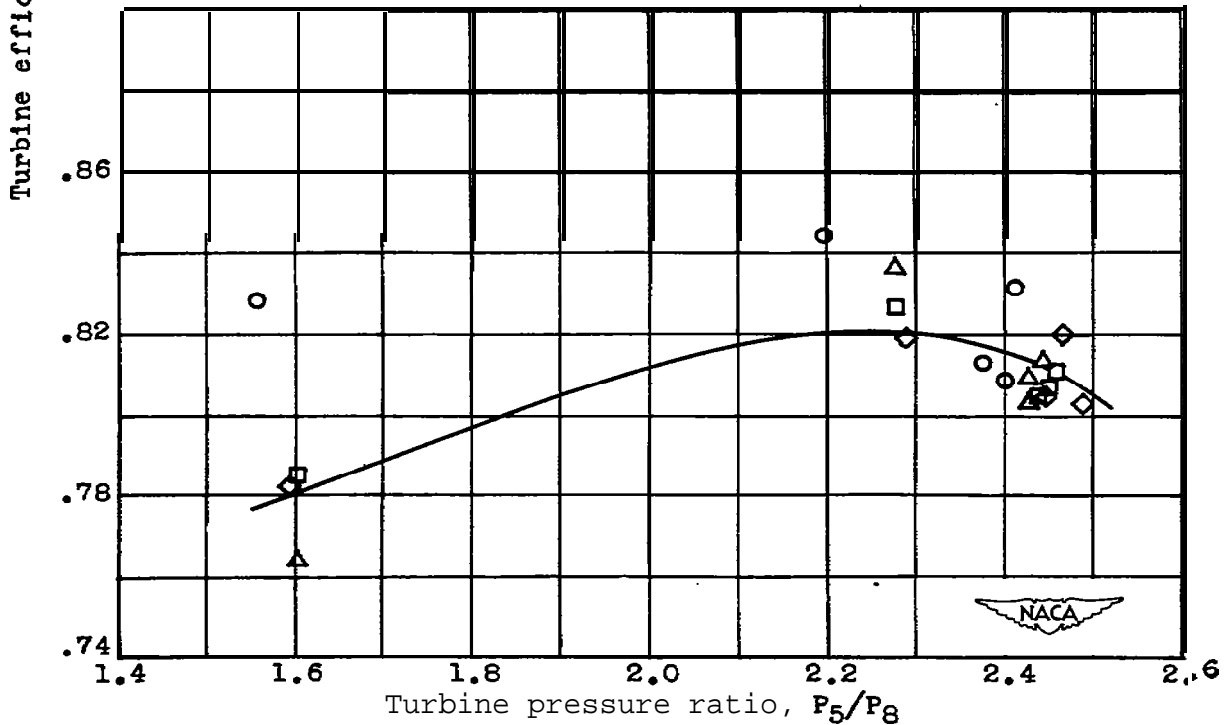


Figure 9.- Turbine operating line and plot of turbine pressure ratio against corrected turbine speed for three tail pipes at simulated altitude of 20,000 feet and ram pressure ratio of 1.03. Turbine speed and gas flow corrected to NACA standard atmospheric conditions at sea level.

641



(a) Tail pipe 2.



(b) Tail pipe 3.

Figure 10.- Effect of altitude on turbine efficiency at a ram pressure ratio of 1.03 for two different tail pipes.

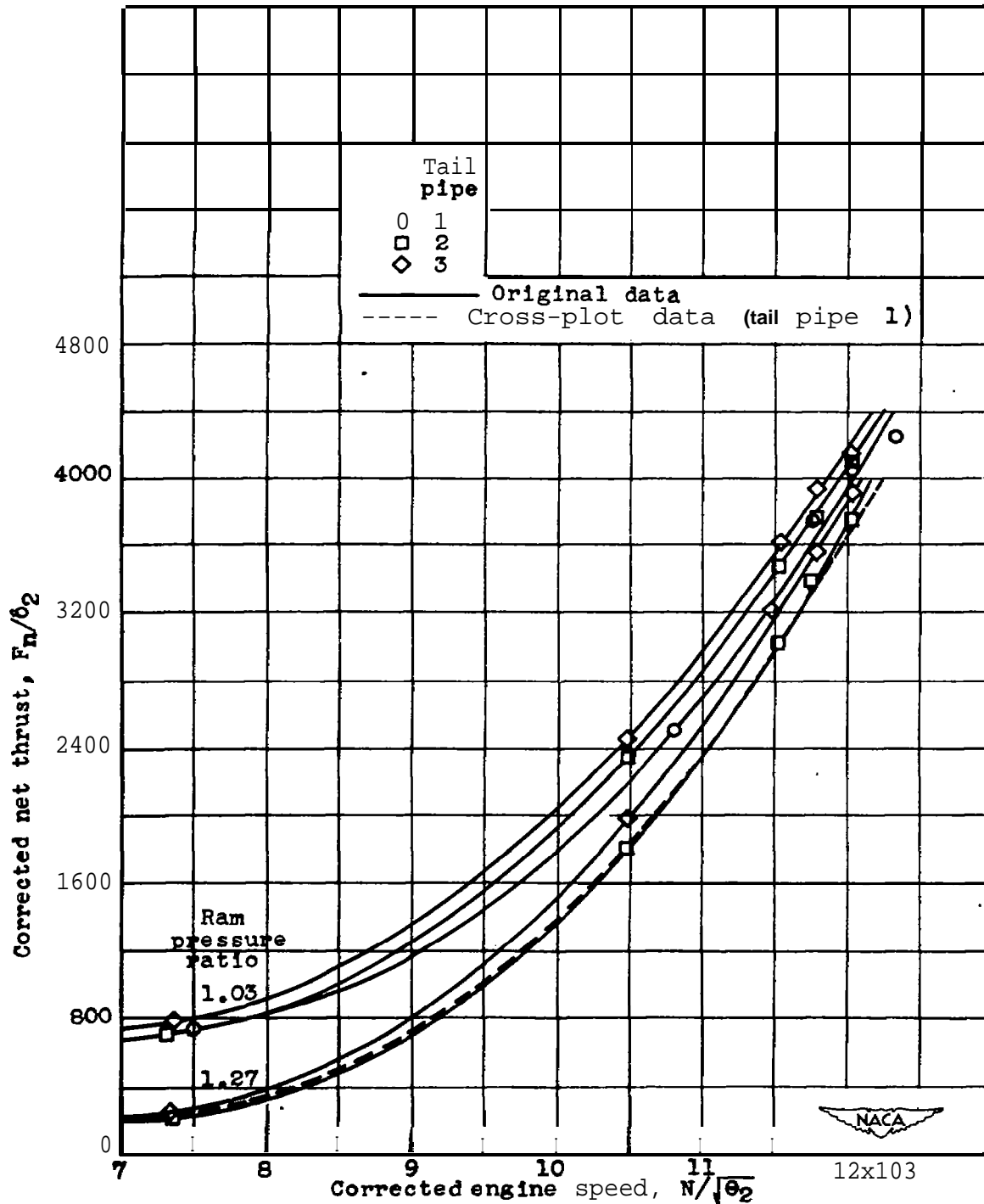


Figure 11.- Effect of tail-pipe design on corrected net thrust for two ram pressure ratios at a simulated altitude of 20,000 feet. Net thrust and engine speed corrected to NACA standard atmospheric conditions at sea level.

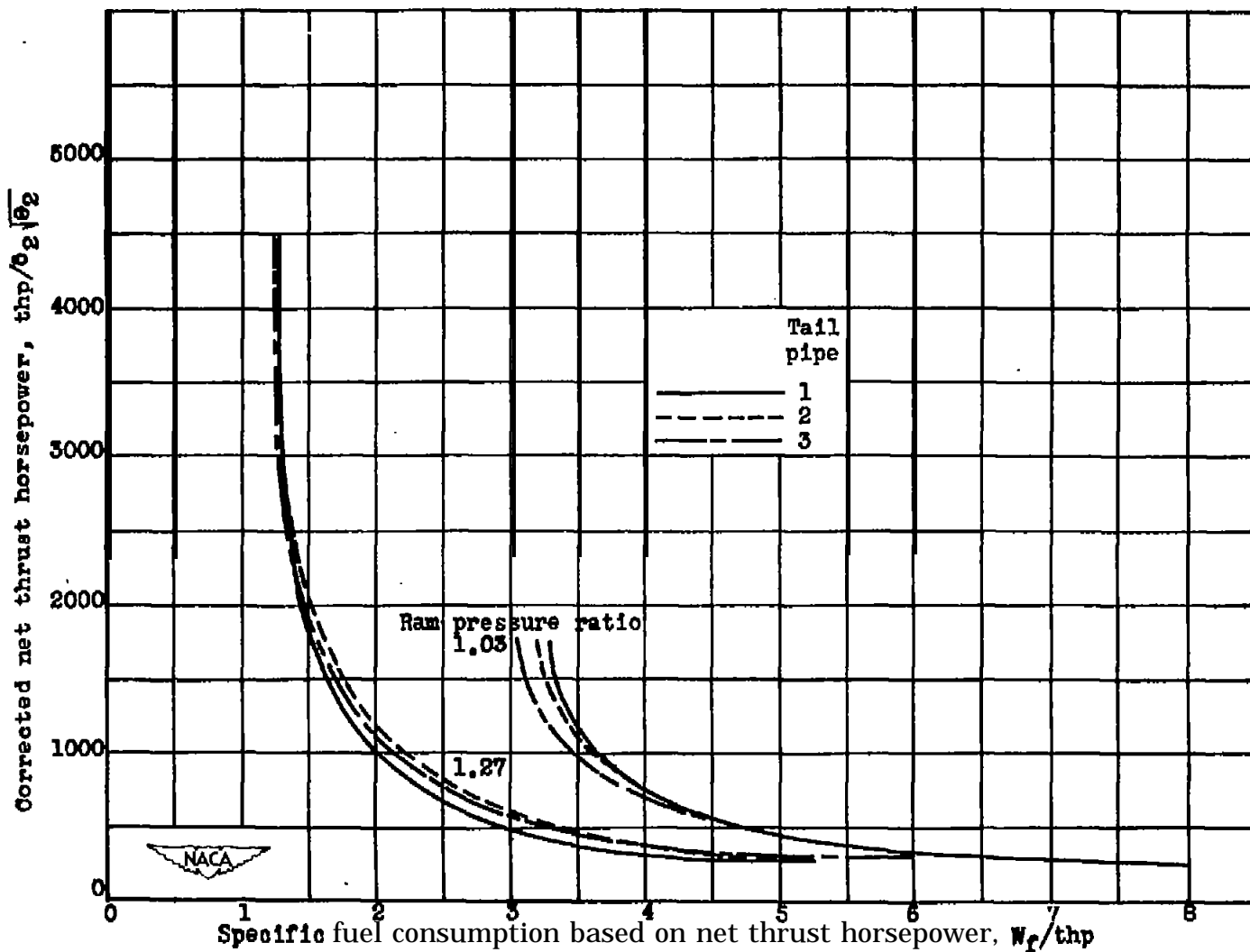


Figure 12.- Effect of tail-pipe design on relation between corrected net-thrust horsepower and specific fuel consumption for two ram pressure ratios at simulated altitude of 20,000 feet. Net-thrust horsepower corrected to NACA standard atmospheric conditions at sea level.

NASA Technical Library



3 1176 01435 5748